

# The Oxidation Behavior of Aluminide-Coated $\gamma'/\delta$ Directional Eutectics

H. C. BHEDWAR, R. W. HECKEL, AND D. E. LAUGHLIN

The relationship between the process variables and the property of oxidation resistance was investigated for aluminide-coated  $\gamma'/\delta$  directional eutectics by the control of the surface composition and the coating microstructure. The oxidation behavior of coated and uncoated substrates was found to belong to three main groups, depending on the surface composition of the coated or uncoated substrate prior to oxidation and irrespective of the manner in which the coating was processed. The coatings with surface composition in Group I formed protective external scales of  $\text{Al}_2\text{O}_3$ ; those with surface compositions in Group II formed nonprotective external scales of niobium-rich oxides; those substrates with surface compositions in Group III formed nonprotective external scales of  $\text{NiO}$ . The oxidation behavior within each group is herein explained in terms of the coating microstructure. Coatings that possessed a single-phase surface layer demonstrated better oxidation resistance than those with a two-phase lamellar morphology.

THE overall direction followed by alloy developers has been toward enhancement of the mechanical properties of directional eutectics. Consequently, a paucity of research exists in other areas. If these materials are to be seriously considered as turbine blade candidates, their oxidation and hot-corrosion behavior is of utmost importance and needs to be explored thoroughly. Only recently has the oxidation behavior of directional eutectics received attention.<sup>1-4</sup> These studies have shown that alloys in the Ni-Al-Nb system ( $\gamma'/\delta$  eutectics) and in the Ni-Al-Nb-Cr system ( $\gamma - \gamma'/\delta$  eutectics), oxidize preferentially along the  $\delta$ -phase lamellae,<sup>1,2</sup> resulting in poor oxidation behavior. Protective coatings are necessary for these alloys to function adequately for long periods of time at high temperatures.

The nature of the protection system depends on the specific application in which the substrate component is to be used. In general, high-operating temperature surfaces (e.g., gas path surfaces on airfoils) require sophisticated oxidation/corrosion-resistant coatings, whereas low-operating temperature surfaces (internal cooling passages and possibly blade roots) can be protected by conventional coatings. It has been demonstrated that overlay coatings of the Ni-Cr-Al-Y and Co-Cr-Al-Y type provide superior oxidation resistance at temperatures above 1150 °C.<sup>3,4</sup> However, these coatings are applied by the electron-beam physical vapor deposition (PVD) process<sup>3,5</sup> which is a line-of-sight coating. Consequently deposition is restricted only to areas accessible to the vapor beam. Internal cooling passages, for instance, cannot be coated by this method and require alternative processes.

Aluminide coatings have been used for a number of years as an efficient, low-cost means for oxidation resistance at temperatures below 1100 °C.<sup>6-8</sup> Briefly, aluminide coatings are applied by diffusing aluminum into the surface of the substrate so as to convert it to an aluminide. Upon oxidation, the surface aluminide layer oxidizes to form a tenacious layer of aluminum oxide which serves as a primary barrier against further oxidation. While the aluminide layers may be formed by a variety of methods,<sup>7,9</sup> the pack-cementation method is the most commonly used technique for large-scale, batch-processing of turbine hardware. Even if new coating systems come into use as demands for engine performance increase, the relatively low-cost aluminide coatings will continue to be used for temperatures up to 1000 °C.<sup>3</sup>

One way to improve aluminide coating technology for specific applications is to obtain an understanding of the effect of the (pack cementation) variables on the coating microstructure\* of the substrate ( $\gamma'/\delta$

---

\* Coating microstructure as used in the present paper means the identity, sequence and the morphology of the phase layers in the coatings.

directional eutectics) and then to examine the effect of the coating microstructure on a specific property of interest—in the present study, the oxidation behavior. The effect of the processing variables on the coating microstructure was studied in a previous paper.<sup>10</sup> It was shown that a spectrum of coating microstructures could be obtained depending on the choice of the process variables, viz., the aluminizing and the homogenizing temperatures, the homogenizing time and the activity of aluminum in the coating pack. The purpose of this paper is to correlate the oxidation behavior of  $\gamma'/\delta$  directional eutectics to the coating microstructure of these alloys and thereby demonstrate that oxidation-resistant coatings can be produced by a proper selection of the coating microstructure. Although only one coating-substrate system was used, the conclusions drawn from the present study are expected to apply to other aluminide-coated directional eutectics.

---

H. C. BHEDWAR, formerly Graduate Student, Department of Metallurgy and Materials Science, Carnegie-Mellon University, Pittsburgh, PA 15213, is now with E. I. du Pont de Nemours & Company, Inc., Engineering Technology Laboratory, Wilmington, DE 19898. R. W. HECKEL is Professor, Department of Metallurgical Engineering, Michigan Technological University, Houghton, MI 49931. D. E. LAUGHLIN is Associate Professor, Department of Metallurgy and Materials Science, Carnegie-Mellon University, Schenley Park, Pittsburgh, PA 15213.

Manuscript submitted November 6, 1978.

## EXPERIMENTAL PROCEDURE

Rectangular sections (1.0 cm × 1.0 cm × 0.3 cm) were cut from a directionally-solidified  $\gamma/\delta$  alloy (nominal composition: 75 pct Ni-9.9 pct Al-15.1 pct Nb). The specimens were ground, degreased and aluminized using the pack-cementation process.<sup>7,11,12,13</sup> Some of the details of the aluminizing treatment are given in Table I. Other details of the experimental procedure are given elsewhere.<sup>14</sup> A majority of the aluminized substrates were given high-temperature, long-term anneals in argon (homogenization) in order to obtain different coating microstructures. Table II summarizes the various processing conditions, the surface phases obtained, and their mean phase composition.

Samples with various coating microstructures obtained by the aluminization and the homogenization processes were oxidized at 900 and 1140 °C in air at a pressure of one atm. The oxidation kinetics were determined by continuous weight-gain vs time measurements using a Cahn electrobalance (Model RG-2000) having a maximum capacity of 2 g and a sensitivity of  $\pm 5 \mu\text{g}$ . The balance was situated over a mullite tube (the oxidation chamber) and connected to it by an O-ring seal and a 40/35 standard taper joint. The system was such that the substrates could be oxidized in static atmospheres of 1 atm pressure. The substrate to be oxidized was suspended from the balance by a Pt/10 pct Rh wire.

The oxidation runs were started by prior positioning of the mullite tube immediately above the furnace and then mechanically raising the furnace (Lindberg crucible furnace—5600 series) so that the tube was in the hot zone. The desired temperature, as measured by a chromel-alumel thermocouple mounted in contact with the mullite tube, was attained in about 12 min. The temperature during an oxidation run varied by less than  $\pm 3^\circ\text{C}$ . Upon termination of the experiment, the furnace was quickly lowered and removed.

A combination of metallography, electron microprobe analyses (EMPA) (both wavelength-dispersive (WDA) and energy-dispersive analyses (EDA)) and X-ray diffraction techniques (XRD) were used for phase identification in both the coating microstructures and the oxide layers. Microprobe intensities from three line emissions (Ni, K $\alpha$ , Al K $\alpha$  and Nb L $\alpha$ ) were

recorded by point and line counting performed parallel to the surface at successive steps approximately equidistant from it. The raw intensities were corrected for background, dead-times and drift, and then converted to concentration values using the alpha-coefficient method.<sup>15</sup>

## EXPERIMENTAL RESULTS

The data in Table III show that the mean surface compositions of coated and uncoated  $\gamma/\delta$  directional eutectics, obtained by different processing conditions, fall into three groups depending on their external oxide scale and their relative oxidation kinetics. Surface compositions belonging to Group I (coated substrates) formed a protective external scale of  $\text{Al}_2\text{O}_3$  with parabolic weight gains at 1140 °C in air after 28 h of 0.16 to  $0.31 \text{ mg}^2\text{cm}^{-4}$ ; those belonging to Group II (coated substrates) formed an external layer of niobium-rich oxide and an internal layer of  $\text{Al}_2\text{O}_3^*$  with parabolic

\* Internal layers must not be confused with internally oxidized layers. The former are continuous, dense layers formed below the external scale. The latter are discrete oxide particles precipitated in the metal.

weight gains of 4.5 to  $13.5 \text{ mg}^2\text{cm}^{-4}$ . Surface compositions belonging to Group III (uncoated substrates) formed an external layer of NiO with internal layers of niobium-rich oxides and  $\text{Al}_2\text{O}_3$ , and showed parabolic weight gains of about  $180 \text{ mg}^2\text{cm}^{-4}$ .

Figure 1 shows the surface composition data of Table III plotted on 900 and 1140 °C ternary isotherms. The purpose of the dashed lines in Fig. 1 is to denote *roughly* the three classification groups. These lines are not precise determinations of the compositional limits of the three groups and should not be so construed. The mean surface compositions of the variously treated samples are plotted on the ternary phase diagram. This will be referred to later when it will be shown that composition and microstructure together with the ability to form desirable oxide phases, control the oxidation behavior of coated and uncoated  $\gamma/\delta$  directional eutectics.

### A. Group I Oxidation Behavior

The oxidation kinetics for all surface compositions belonging to Group I in Fig. 1 eventually obeyed a

Table I. Aluminizing Times, Temperatures and the Composition for High- and Low-Aluminum Activity Packs

Type of Coating	Aluminizing Temperature (°C)	Aluminizing Time (hr)	Pack Composition (weight-percent)			
			Inert Filler $\text{Al}_2\text{O}_3$ (−325 mesh)	Activator $\text{NH}_4\text{Cl}$	Pure Aluminum (−325 mesh)	Aluminum Alloy 45 at. pct Ni-55 at. pct Al (−325 mesh)
High-Aluminum-Activity Pack	900	0.33	72.0	3.0	25.0	—
	1140	0.5	94.0	3.0	3.0	—
Low-Aluminum-Activity Pack	900	10.0	72.0	3.0	—	25.0
	1140	1.0	72.0	3.0	—	25.0

**Table II. The Surface Phases and Their Mean Composition During the Aluminizing and the Homogenizing Treatments on Coated  $\gamma'/\delta$  Directional Eutectics**

Treatment	Aluminum Activity of the Pack	Aluminizing Temperature, °C	Homogenizing Time,* h	Surface Phases	Mean Composition	
Aluminizing	High-Aluminum-Activity Pack	900	—	Ni <sub>2</sub> Al <sub>3</sub> + NbAl <sub>3</sub>	29.5 Ni-5.5 Nb-65.0 Al	
		1140	—	Al-rich $\beta$ + NbAl <sub>3</sub>	37.0 Ni-6.0 Nb 57.0 Al	
	Low-Aluminum-Activity Pack	900	—	$\beta$	46.1 Ni-0.8 Nb-53.1 Al	
		1140	—	$\beta$	50.5 Ni-0.05 Nb-49.45 Al	
	Homogenizing	High-Aluminum Activity Pack	900	16.25	Ni <sub>2</sub> Al <sub>3</sub> + NbAl <sub>3</sub>	32.7 Ni-6.2 Nb-61.1 Al
				50	Al-rich $\beta$ + NbAl <sub>3</sub>	39.8 Ni-6.2 Nb-54 Al
150				Ni-rich $\beta$ + $\eta$	57.4 Ni-5.6 Nb-37 Al	
		1140	1	Al-rich $\beta$ + NbAl <sub>3</sub>	41.2 Ni-5.3 Nb-53.5 Al	
			3	Al-rich $\beta$ + NbAl <sub>3</sub>	43.2 Ni-4.8 Nb-52 Al	
			50	Ni-rich $\beta$	59.7 Ni-3.3 Nb-37 Al	
Low-Aluminum-Activity Pack	1140	1	$\beta$	52 Ni-4.2 Nb-43.8 Al		
		50	Ni-rich $\beta$ + $\eta$	54.8 Ni-12.1 Nb-33.1 Al		
		150	Ni-rich $\beta$ + $\eta$	57.4 Ni-9.0 Nb-33.6 Al		

\*Homogenizing temperature same as aluminizing temperature.

**Table III. The Mean Surface Composition, the Oxide Phases and Parabolic Weight-Gains of Coated and Uncoated  $\gamma'/\delta$  Directional Eutectics**

Aluminizing Temperature, °C	Aluminum Pack Activity	Homogenizing Temperature, °C	Homogenizing Time, h	Group I	Group II	Group III
900	High	—	—	29.5 Ni-5.5 Nb-65 Al		
1140	High	—	—	37.0 Ni-6.0 Nb-57 Al		
900	Low	—	—	46.1 Ni-0.8 Nb-53.1 Al		
1140	Low	—	—	50.5 Ni-0.05 Nb-49.45 Al		
900	High	900	16.25	37.7 Ni-6.2 Nb-61.1 Al		
900	High	900	50	39.8 Ni-6.2 Nb-54 Al		
1140	High	1140	3	43.2 Ni-4.8 Nb-52 Al		
1140	High	1140	50	59.7 Ni-3.3 Nb-37 Al		
1140	Low	1140	1	52 Ni-4.2 Nb-43.8 Al		
900	High	900	150	—	57.4 Ni-5.6 Nb-37 Al	
1140	Low	1140	50	—	54.8 Ni-12.1 Nb-33.1 Al	
1140	Low	1140	150	—	57.4 Ni-9.0 Nb-33.6 Al	
—	—	—	—	—	—	75 Ni-15.1 Nb-9.9 Al
				External Scale	Al <sub>2</sub> O <sub>3</sub>	Niobium-rich oxide
				Oxides Phases		NiO
				Internal Layer	Traces of niobium-rich oxides at early times	NiNb <sub>2</sub> O <sub>6</sub> , AlNbO <sub>4</sub> , Al <sub>2</sub> O <sub>3</sub> only at 1140 °C oxidation temperature, NiO at 900 °C
				Parabolic weight gains in air at 1140 °C after 28 h (mg <sup>2</sup> cm <sup>-4</sup> )	0.16 to 0.31	4.5 to 13.5
						180

parabolic rate law. Usually, this rate law was followed virtually from the beginning of the weight-gain measurements, although in some cases, conformation was not evident until about 3 h of oxidation. Typical

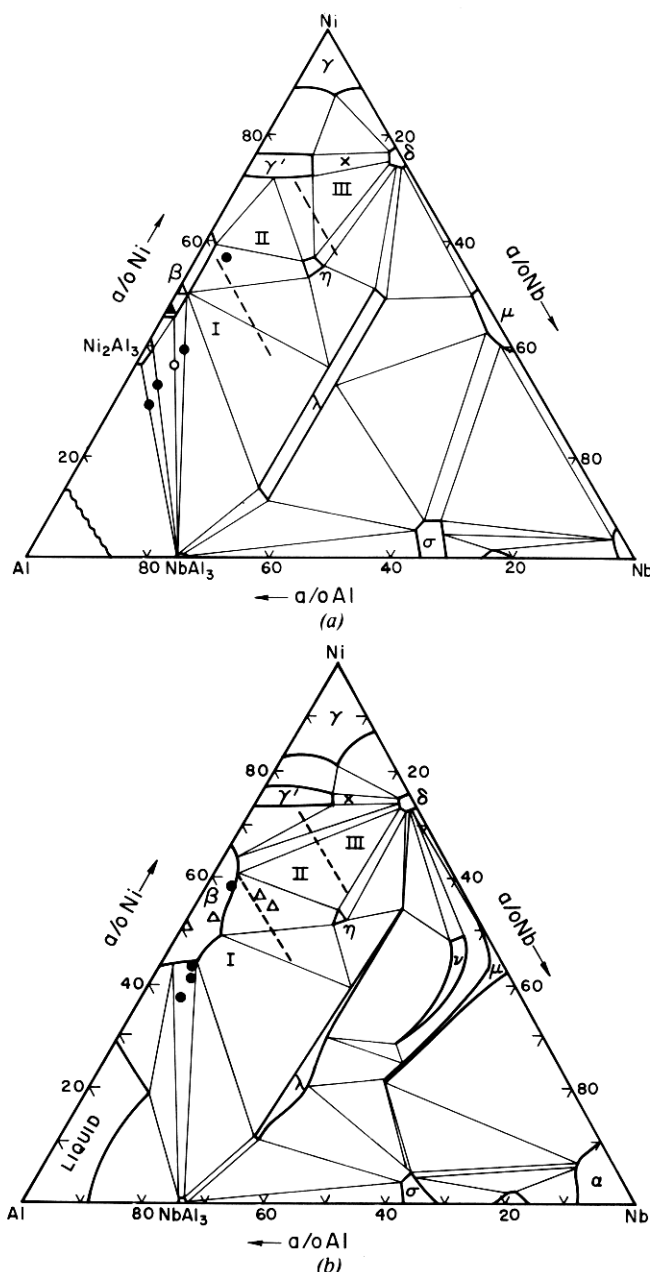


Fig. 1—(a) The 900 °C isotherm showing the compositional limits for the three oxidation mechanisms of uncoated and aluminide-coated  $\gamma'/\delta$  directional eutectics. The symbols indicate the surface composition of the coatings and the uncoated substrate. ● Coatings deposited by high-aluminum-activity packs at 900 °C and oxidized at 900 °C; ○ Coatings deposited by high-aluminum-activity packs at 1140 °C and oxidized at 900 °C; ▲ Coatings deposited by low-aluminum-activity packs at 900 °C and oxidized at 900 °C; △ Coatings deposited by low-aluminum-activity packs at 1140 °C and oxidized at 900 °C; × Uncoated substrates oxidized at 900 °C. (b) The 1140 °C isotherm showing the compositional limits for the three oxidation mechanisms of uncoated and aluminide-coated  $\gamma'/\delta$  directional eutectics. The symbols indicate the surface composition of the coating and the uncoated substrate. ● Coatings deposited by high-aluminum-activity packs at 1140 °C and oxidized at 1140 °C; △ Coatings deposited by low-aluminum-activity packs at 1140 °C and oxidized at 1140 °C; × Uncoated substrates oxidized at 1140 °C.

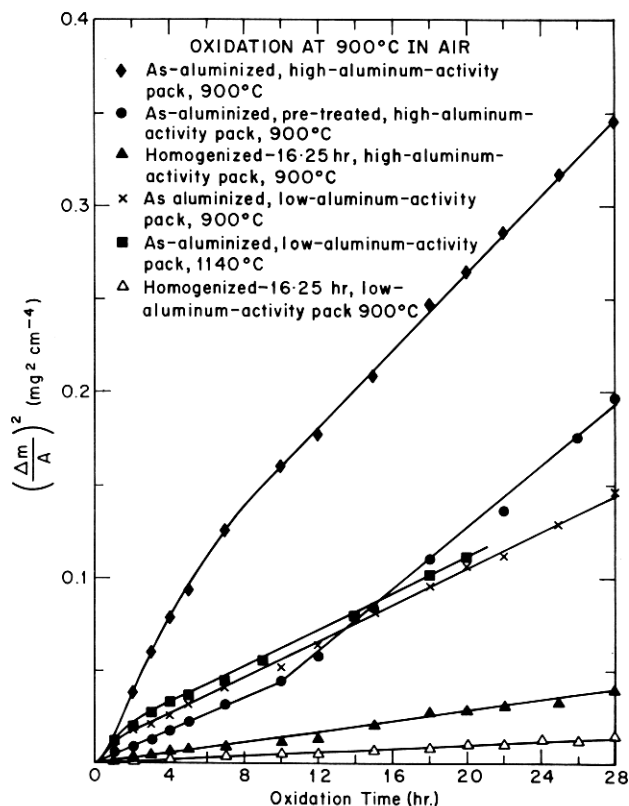


Fig. 2—Typical weight-gain data for Group I coatings oxidized at 900 °C in air.

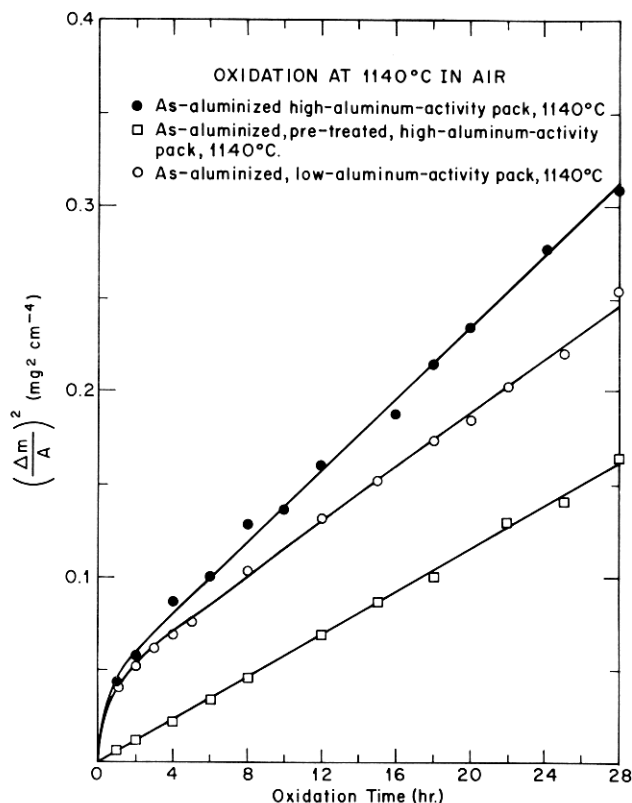


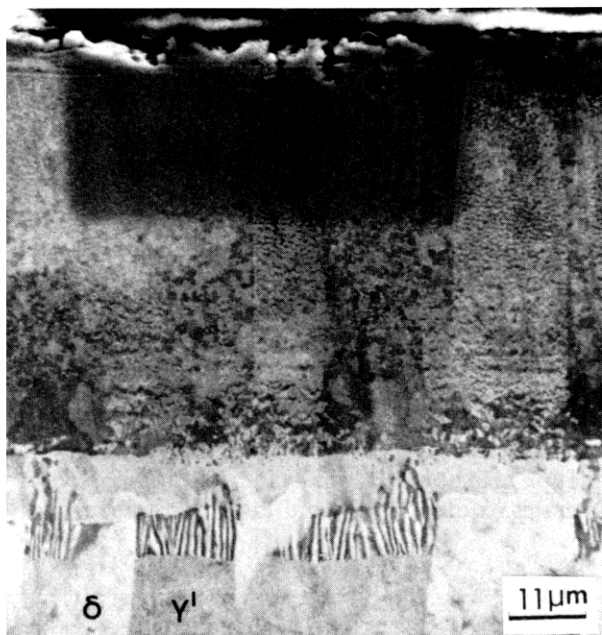
Fig. 3—Typical weight-gain data for Group I coatings oxidized at 1140 °C in air.

weight-gain measurements are presented in Figs. 2 and 3, corresponding to oxidation temperatures of 900 and 1140 °C, respectively.

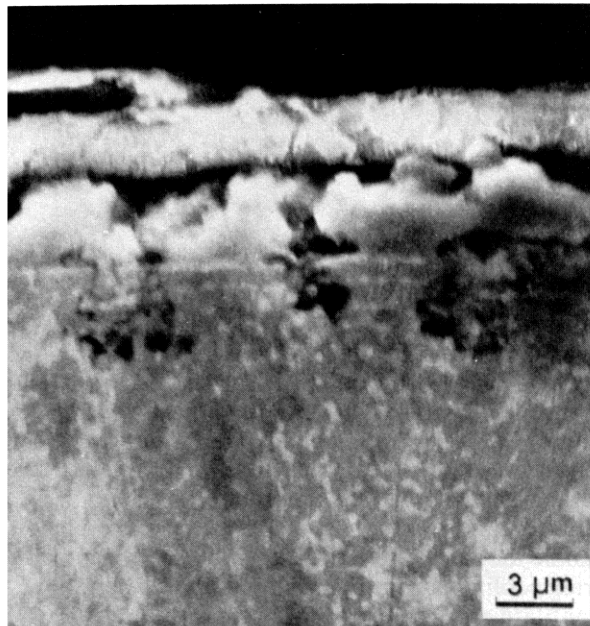
The weight-gain measurements plotted in Figs. 2 and 3 show that substrates with coatings deposited by low-aluminum-activity packs at 900 and 1140 °C had slower kinetics than those deposited by high-aluminum-activity packs. However, when the high-aluminum-activity pack coatings deposited at 900 and 1140 °C were pretreated (by short anneals in argon—0.5 h at 900 °C prior to the weight-gain measurements), the

oxidation kinetics decreased substantially. When a homogenizing treatment was given to coatings deposited by high-aluminum-activity packs at 900 °C, the oxidation kinetics decreased even further (Fig. 2). However, as will be shown in the section on Group II oxidation behavior, when coatings deposited by high-aluminum-activity packs at 1140 °C were given a homogenizing treatment at 1140 °C, the oxidation kinetics increased.

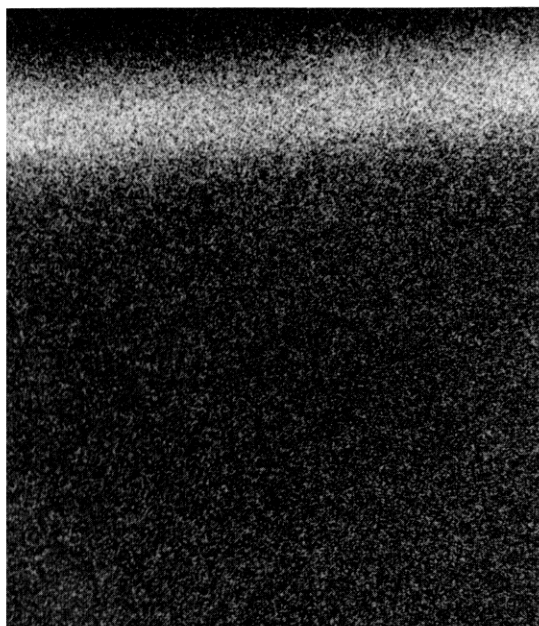
A typical oxidized coating exhibiting a two-phase lamellar morphology and belonging to Group I is



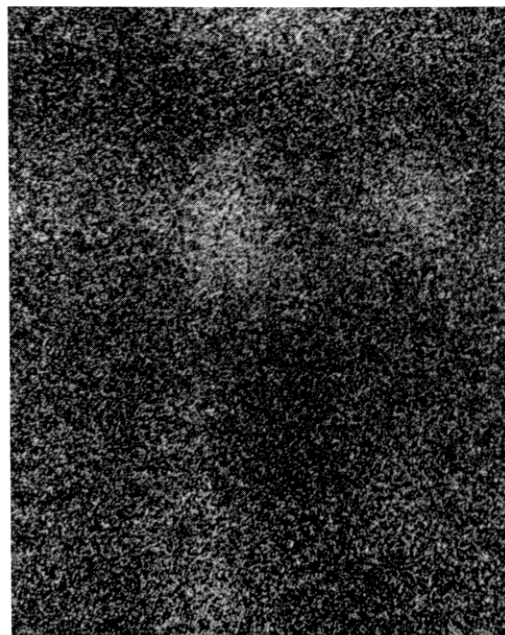
(a)



(b)

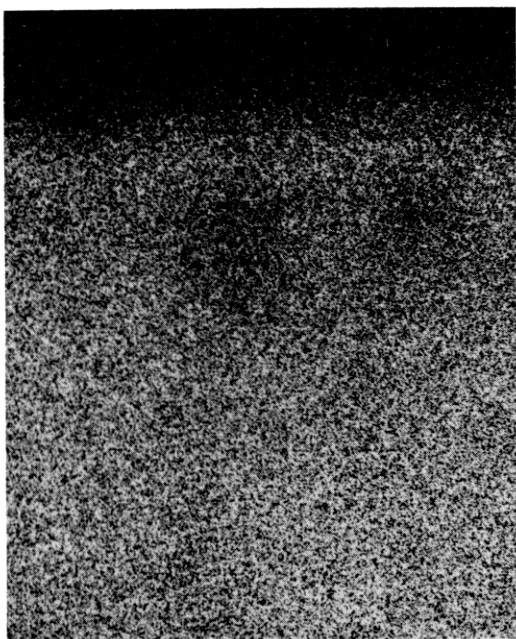


(c)



(d)

Fig. 4—(a) Microstructure of a Group I coating showing the two-phase lamellar morphology in the coating. (b) Microstructure of a Group I coating deposited by a high-aluminum-activity pack at 900 °C, homogenized for 16.25 h at 900 °C and oxidized for 53 h at 900 °C (secondary electron image). (c) Aluminum X-ray image. (d) Niobium X-ray image. (e) Nickel X-ray image.



(e)  
Fig. 4—Continued.

shown in Fig. 4. Only an external scale developed on this group of coatings and, although there was no evidence of oxide spall on cooling to room temperature, the scale in some cases appeared to be separated from the substrate. It is assumed that the scale separation occurred during isothermal oxidation even though it is possible that the scale separation may have occurred during cooling or during metallographic preparation. Quantitative EDA measurements and surface X-ray diffraction of the scale confirmed that the external scale consisted of  $\text{Al}_2\text{O}_3$ . X-ray images for nickel, niobium and aluminum radiation are shown in Fig. 4.

### B. Group II Oxidation Behavior

Typical weight-gain vs time curves for coatings with surface compositions in Region II of Fig. 1 are presented in Fig. 5. Initially, the coatings underwent rapid weight gains but eventually the oxidation kinetics tended to approach parabolic behavior. As seen in Fig. 5, one of the weight-gain curves showed "breakaway" oxidation behavior which is a possible consequence of scale-cracking. Coatings deposited by low-aluminum-activity packs and given homogenizing treatments demonstrated slower oxidation kinetics than those deposited by high-aluminum-activity packs and homogenized for the same time at the same temperature.

A typical oxidized coating belonging to Group II is shown in Fig. 6. Two distinct layers were identified on the surface of the oxidized coating. An external layer consisting of a niobium-rich oxide (the precise oxide phase could not be identified) and an internal layer consisting solely of  $\text{Al}_2\text{O}_3$ . X-ray images of nickel, niobium and aluminum are shown in Fig. 6.

### C. Group III Oxidation Behavior

The oxidation kinetics for substrates having surface compositions belonging to Region III in Fig. 1 are shown in Fig. 7. These substrates were uncoated and consequently their surface compositions corresponded to the mean composition of the substrate. The oxidation kinetics obeyed a parabolic rate law with parabolic constants of  $1.7 \times 10^{-10} \text{ g}^2 \text{ cm}^{-4} \text{ s}^{-1}$  at  $900^\circ \text{C}$  and  $1.6 \times 10^{-9} \text{ g}^2 \text{ cm}^{-4} \text{ s}^{-1}$  at  $1140^\circ \text{C}$ . It was found more convenient to use weight gain after a specific oxidation time (16 h, in the present study) as a means of comparing the oxidation behavior with other studies reported in the literature. In the present study, the weight gain after 16 h of oxidation at  $900^\circ \text{C}$  was  $3.7 \text{ mg cm}^{-2}$  and  $10.2 \text{ mg cm}^{-2}$  at  $1140^\circ \text{C}$ . These values are plotted in Fig. 8 together with those obtained in the literature. The values obtained in this study compare very favorably with those obtained by other workers and can serve as base-line data for comparison with the studies on the coated substrates.

Oxidation at 900 and  $1140^\circ \text{C}$  produced an external scale of NiO which spalled on cooling to room temperature. An internal zone was present on substrates oxidized at 900 and  $1140^\circ \text{C}$ . At  $900^\circ \text{C}$ , the internal zone consisted of  $\text{NiNb}_2\text{O}_6$  and islands of almost pure nickel, as seen in Fig. 9; however, at  $1140^\circ \text{C}$  the internal zone consisted of  $\text{NiNb}_2\text{O}_6$ ,  $\text{AlNbO}_4$  and  $\text{Al}_2\text{O}_3$ , Fig. 10. X-ray images of nickel, aluminum and niobium radiation are shown in Figs. 9 and 10 for uncoated substrates oxidized at 900 and  $1140^\circ \text{C}$ , respectively.

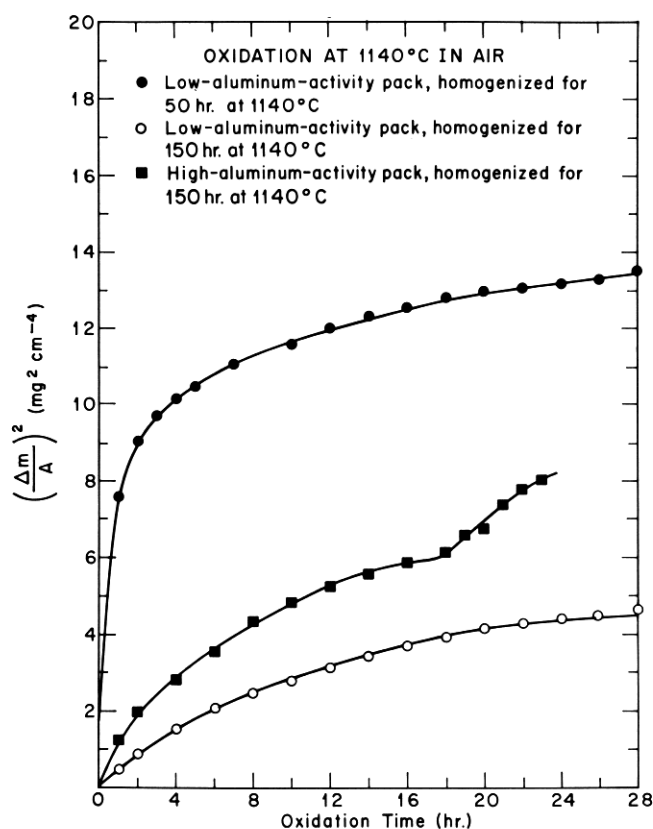


Fig. 5—Typical weight-gain data for Group II coatings oxidized at  $1140^\circ \text{C}$  in air.

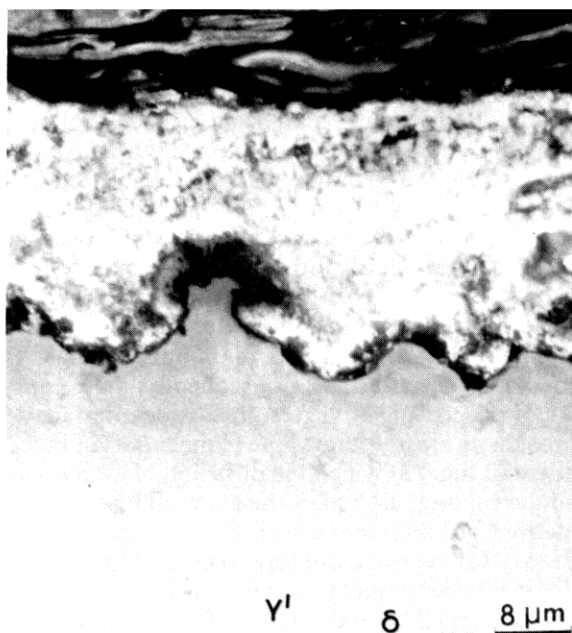


## DISCUSSION

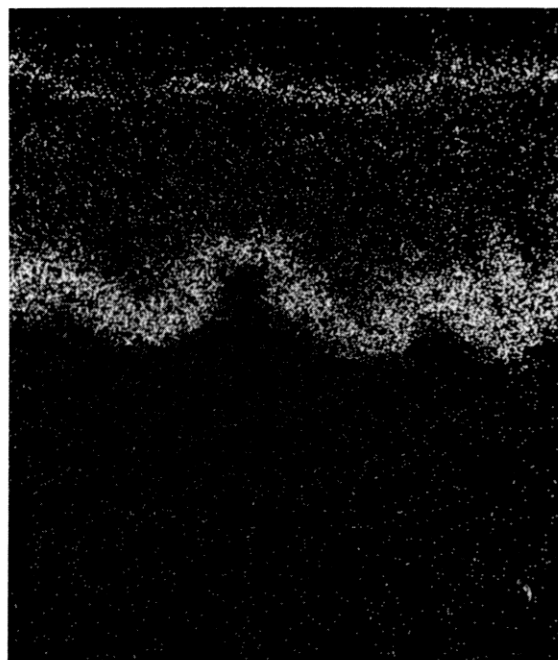
The data in Table III show that, although a variety of processing conditions were used to form coatings, their oxidation behavior fell into two groups (the third group constituted uncoated substrates). Each group was characterized by specific oxide phases and oxidation kinetics. The factors controlling the oxidation kinetics and formation of the oxide phases are discussed in the following sections.

Wagner<sup>16</sup> has shown that a less noble element will

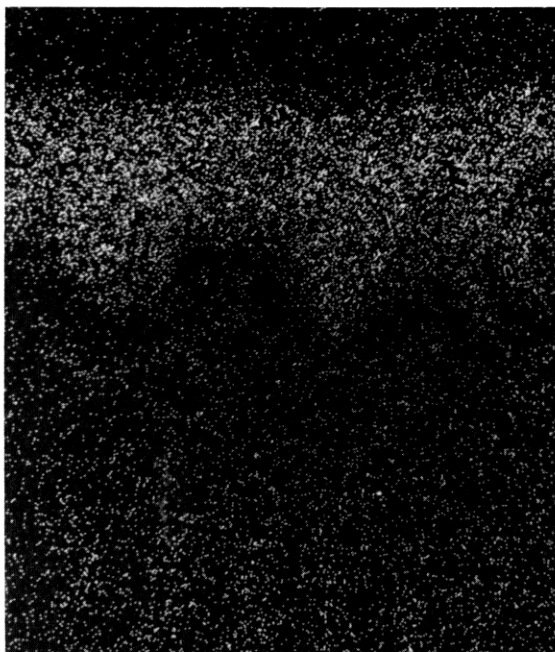
form a dense, external oxide only if the mole fraction of its oxide is greater than some critical amount, *i.e.*,  $N_{MO} > N_{MO}^*$ . If this criterion is not met, a layer of internally oxidized particles will form. The formation and the maintenance of an oxide layer exclusive of the other oxides requires another criterion to be satisfied. The diffusive flux through the alloy of the element  $M$  must be greater than the flux of the element consumed due to oxidation, *i.e.*,  $J_{alloy}^M > J_{oxide}^M$ . If this condition is not met throughout the oxidation process, other oxide phases become stable.



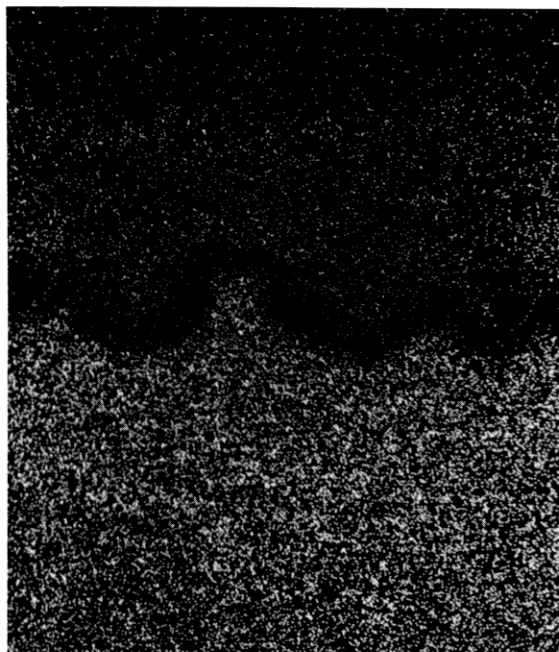
(a)



(b)



(c)



(d)

Fig. 6—(a) Microstructure of a Group II coating deposited by a high-aluminum-activity pack at 1140 °C, homogenized for 15 h at 1140 °C and oxidized for 28 h at 1140 °C (secondary electron image). (b) Aluminum x-ray image. (c) Niobium X-ray image. (d) Nickel X-ray image.

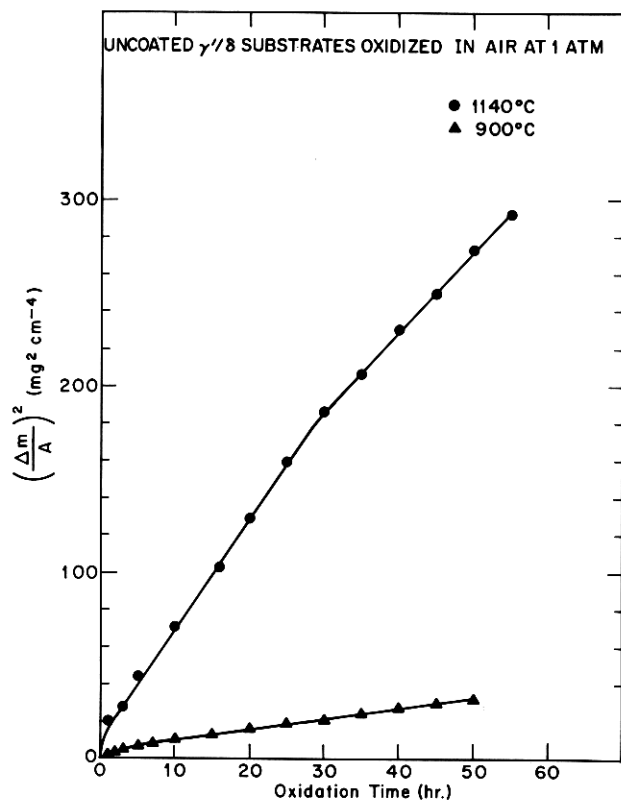


Fig. 7—Typical weight-gain data for Group III substrates oxidized in air at 900 and 1140 °C.

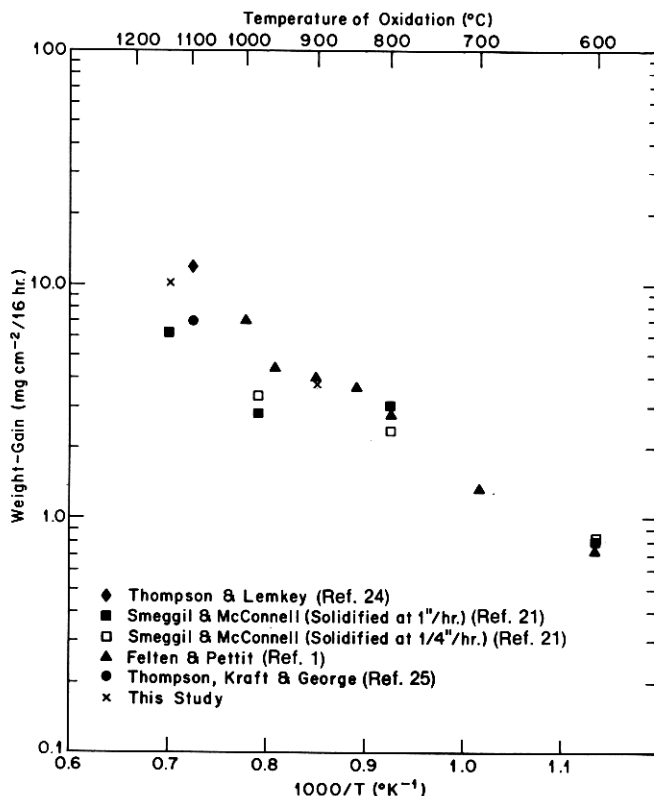


Fig. 8—The weight-gain after 16 h plotted as a function of the reciprocal of the oxidation temperature, as a means of comparing the data from this study with those in the literature.

## A. Group I Oxidation Behavior

i) *The Effect of Surface Composition on the Oxidation Behavior of Coated Directional Eutectics.* The results of Group I coatings show that an external layer of  $\text{Al}_2\text{O}_3$  forms on the surface of the coatings. This indicates that the mole fraction of  $\text{Al}_2\text{O}_3$  precipitated on the surface is greater than the critical mole fraction for external oxidation, i.e.,  $N_{\text{Al}_2\text{O}_3} > N_{\text{Al}_2\text{O}_3}^*$ , and that the initial diffusive flux of aluminum to the coating surface from the interior of the alloy is faster than the diffusive flux of aluminum consumed due to oxidation i.e.,  $J_{\text{oxide}}^{\text{Al}} > J_{\text{coating}}^{\text{Al}}$ . Under these conditions the  $\text{Al}_2\text{O}_3$  is stable as long as the oxygen pressure in the gas phase is above the equilibrium value for the formation of  $\text{Al}_2\text{O}_3$ .

In view of the results obtained with Group I coatings, an oxidation mechanism can be described as follows. During the early stages of oxidation, aluminum is removed from the coating surface and converted to the oxide so rapidly that a concentration gradient is created in the coating adjacent to the coating/oxide interface. The depletion of aluminum at the coating/oxide interface has a two-fold effect: i) it promotes the diffusion of aluminum from the coating to the coating/oxide interface, ii) it decreases the flux of aluminum through  $\text{Al}_2\text{O}_3$  to the  $\text{Al}_2\text{O}_3$ /gas interface. Consequently, the composition of the coating at the coating/oxide interface approaches a steady state value (concentration independent of time) at which the diffusion of aluminum from the coating just equals the aluminum consumed in oxidation. The maintenance of the aluminum flux is necessary for the exclusive formation of  $\text{Al}_2\text{O}_3$  in the scale since other oxides (e.g., niobium-rich oxides and  $\text{NiO}$ ) will form if the oxygen activity in the gas-phase is high enough to promote their formation.

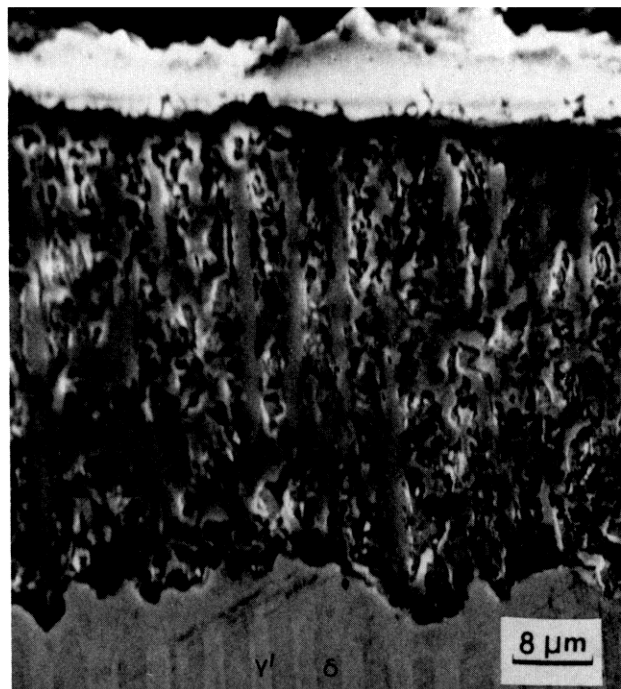
Aluminum can be consumed in oxidation by the diffusion of either aluminum atoms or oxygen atoms through the  $\text{Al}_2\text{O}_3$  scale. Which of these occurs can be determined in principle by placing inert markers on the surface of the unoxidized specimen and noting their ultimate location in the oxide scale.<sup>17</sup> However, marker studies could not be performed in the present research due to the fragile nature of the  $\text{Al}_2\text{O}_3$  scale. Nevertheless the findings of other investigators is of help in understanding the relative motion of Al atoms. In particular, structure-sensitive diffusion (grain boundary diffusion) has been shown to be predominant in  $\alpha\text{-Al}_2\text{O}_3$  below 1400 °C<sup>18,19</sup> with an activation energy considerably less than that for interdiffusion in  $\beta$ ,  $\gamma'$  and  $\gamma$  phases in the Ni-Al-Nb system. Consequently, we propose that the polycrystalline  $\text{Al}_2\text{O}_3$  scale which forms on these alloys accommodates grain boundary diffusion. Since oxygen can diffuse through such an  $\text{Al}_2\text{O}_3$  layer at a faster rate than aluminum atoms can diffuse from the interior coatings, we further propose that the oxide forms by the inward motion of oxygen.

ii) *The Effect of Microstructure on the Oxidation Behavior of Coated Directional Eutectics.* It was shown that coatings deposited by low-aluminum-activity packs (nonlamellar, single-phase surface phases) consistently had better oxidation resistance at both the temperatures of oxidation (900 and 1140 °C). The difference in oxidation behavior was more apparent at 900 than at

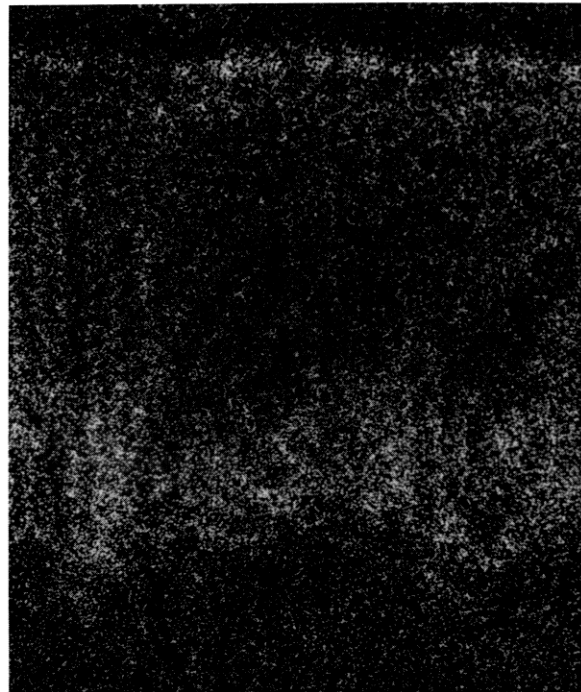


1140 °C, as seen in Figs. 2 and 3. A possible explanation for the better protectiveness of nonlamellar, single-surface phase coatings (low-aluminum-activity packs) is that these coatings had surface layers of the  $\beta$ -phase containing relatively low niobium contents (0.05 to 0.8% Nb), Table II. Coatings deposited by high-aluminum-activity packs, on the other hand, contained two-phase surface layers of  $\text{Ni}_2\text{Al}_3 + \text{NbAl}_3$  at 900 °C

and Al-rich  $\beta + \text{NbAl}_3$  at 1140 °C, Table II. At both temperatures, the niobium content along the  $\delta$ -lamellae could be as high as about 22% Nb. Under such a situation, it is entirely possible that the  $\text{NbAl}_3$ -phase along the  $\delta$ -lamellae initially undergoes rapid oxidation,<sup>20</sup> forming niobium-rich oxides, and then ultimately forming an external scale of  $\text{Al}_2\text{O}_3$ . The rapid oxidation kinetics are apparent in the weight-gain curve for the



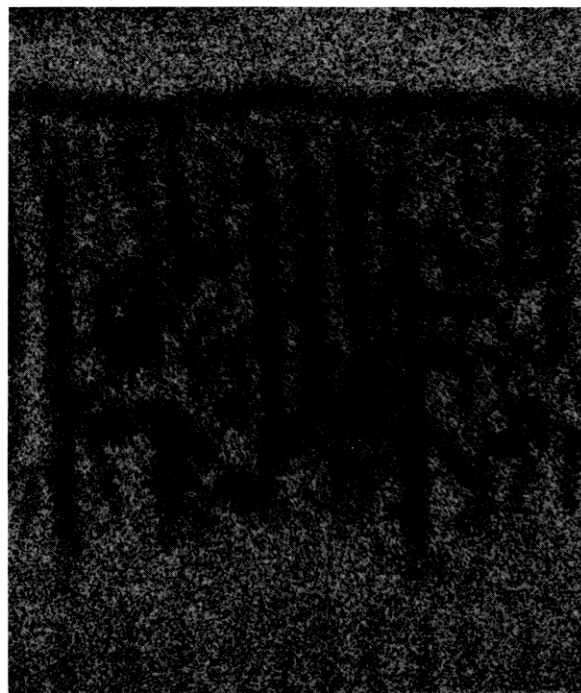
(a)



(b)



(c)



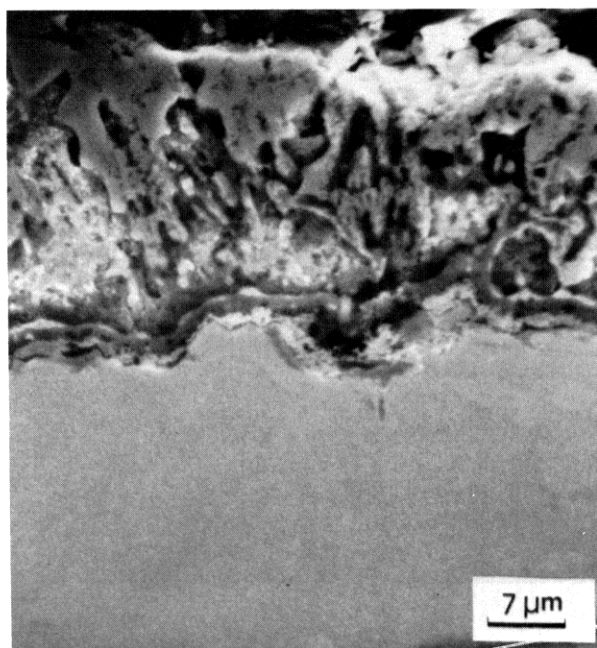
(d)

Fig. 9—(a) Microstructure of an uncoated Group III substrate oxidized for 50 h at 900 °C (secondary electron image). (b) Aluminum X-ray image. (c) Niobium X-ray image. (d) Nickel X-ray image.

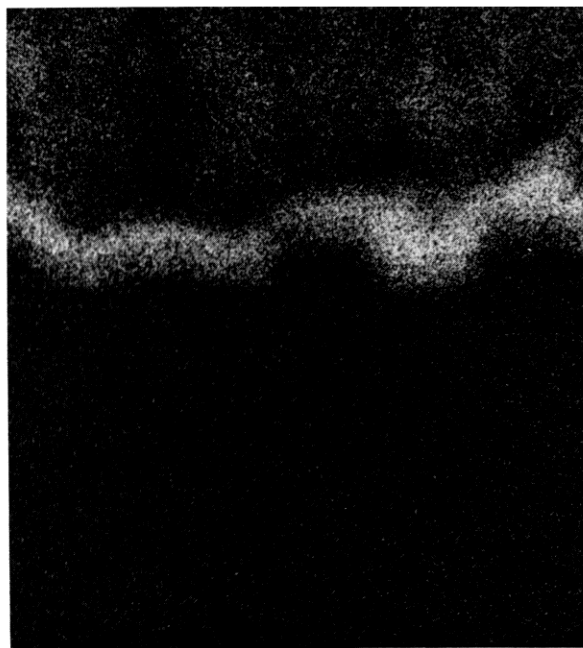
as-aluminized coating deposited by a high-aluminum-activity pack at 900 °C, Fig. 2. Coatings deposited by low-aluminum-activity packs do not have regions of high niobium content and, therefore, do not show rapid initial weight gains, Fig. 2.

iii) *The Effect of Pretreatment on the Oxidation Behavior of Coated Directional Eutectics.* It is possible to reduce oxidation kinetics of aluminized substrates by a pretreatment (argon anneal at 900 °C for 0.5 h) prior to the weight-gain measurements. The purpose of such a treatment is to produce an oxide of the least noble

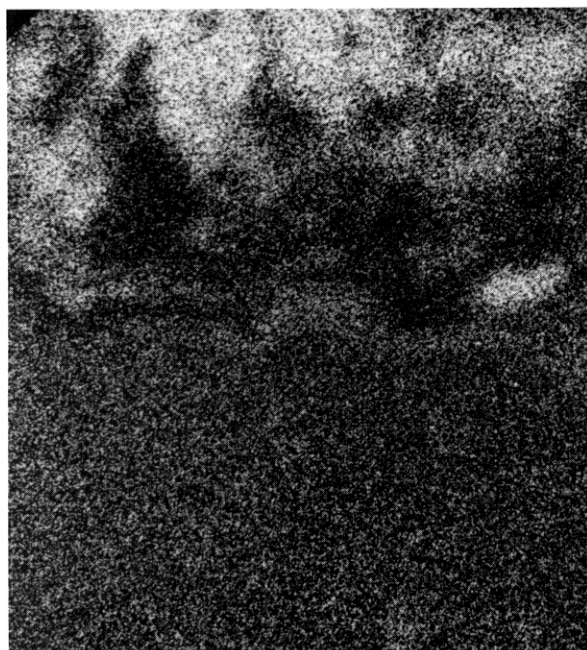
element (by reacting with the O<sub>2</sub> impurity in the argon) in the coating microstructure and thereby increase protection. This treatment differs from long-term homogenization since no structural change occurs in the coating. Kofstad and Hed<sup>22</sup> have shown that low oxygen partial pressures of the gas phase produce protective layers since the oxygen activity in the gas phase is low enough to oxidize the least noble element only. Figure 2 shows that substrates aluminized by a high-aluminum activity pack at 900 °C and oxidized at 900 °C (◆ in Fig. 2) show greater weight gains than



(a)



(b)



(c)



(d)

Fig. 10—(a) Microstructure of an uncoated Group III substrate oxidized for 55 h at 1140 °C (secondary electron image). (b) Aluminum X-ray image. (c) Niobium X-ray image. (d) Nickel X-ray image.

those given a pretreatment prior to oxidation (● in Fig. 2). Similar results are seen in Fig. 3.

High-aluminum-activity pack coatings have a two-phase lamellar morphology ( $\text{Ni}_2\text{Al}_3 + \text{NbAl}_3$  at 900 °C and Al-rich  $\beta + \text{NbAl}_3$  at 1140 °C) Table II. The pretreatment serves to form an initial protective scale over  $\text{NbAl}_3$  (presumably an  $\text{Al}_2\text{O}_3$  scale) rather than the niobium-rich oxide which forms during oxidation in air (see previous section). This  $\text{Al}_2\text{O}_3$  scale tends to reduce weight gains by acting as a protective layer. However, should the protective scale over  $\text{NbAl}_3$  spall or crack, the slope of the weight-gain curve (◆ in Fig. 2) reverts to that of the non-pretreated coating (● in Fig. 2).

## B. Group II Oxidation Behavior

i) *The Effect of Surface Composition on the Oxidation Behavior of Coated Directional Eutectics.* The oxide phases belonging to Group II consisted primarily of an external layer of niobium-rich oxides and a dense internal layer of  $\text{Al}_2\text{O}_3$ , as seen in Fig. 6. The presence of the dense internal layer of  $\text{Al}_2\text{O}_3$  suggests that at early times,  $N_{\text{Al}_2\text{O}_3} > N_{\text{Al}_2\text{O}_3}^*$  and a continuous scale of  $\text{Al}_2\text{O}_3$  formed on the coated substrate. However, as oxidation progressed, aluminum was depleted from the coating/ $\text{Al}_2\text{O}_3$  interface presumably because aluminum was consumed due to oxidation faster than aluminum could diffuse to this interface from the interior of the coating, i.e.  $J_{\text{coating}}^{\text{Al}} < J_{\text{oxide}}^{\text{Al}}$ . The depletion of aluminum reached such a stage that niobium-rich oxides could form. These oxides, though somewhat protective, are not as protective as those in Group I (Figs. 2, 3 and 5).

ii) *The Effect of Microstructure on the Oxidation Behavior of Coated Directional Eutectics.* When the as-aluminized coatings were given a homogenizing treatment at 1140 °C, prior to oxidation, they exhibited Group II behavior. The relatively rapid homogenizing kinetics at 1140 °C (as compared to 900 °C) resulted in the rapid removal (by the outward diffusion of nickel) of the aluminum-rich phases at the surface (see Ref. 10). Consequently, the aluminum concentration at the surface was reduced to such a level that  $\text{Al}_2\text{O}_3$  could no longer form as the external scale  $N_{\text{Al}_2\text{O}_3} < N_{\text{Al}_2\text{O}_3}^*$  and less stable oxides (niobium-rich oxides) formed on the surface.

## C. Group III Oxidation Behavior

Although various aspects of the oxidation mechanism for uncoated  $\gamma/\delta$  substrates have been studied,<sup>1,2,21,22</sup> a discussion based on Wagner's criterion<sup>16</sup> for internal and external oxidation is given here for the sake of completeness. Surface compositions belonging to Group III, typically formed an external layer of NiO and a zone of internal oxidation consisting of  $\text{NiNb}_2\text{O}_6$  and  $\text{AlNbO}_4$ . At 1140 °C, however, an internal layer of  $\text{Al}_2\text{O}_3$  also formed. The directional nature of the substrate was more apparent at 900 °C than at 1140 °C. (See Figs. 9 and 10).

Initially, the surface composition of the substrate is such that NiO forms over the  $\gamma'$ -phase and  $\text{Nb}_2\text{O}_5$  over the  $\delta$  phase. NiO is known to form by the outward

motion of nickel atoms through the oxide<sup>23</sup> whereas  $\text{Nb}_2\text{O}_5$  forms by the inward transport of oxygen.<sup>17</sup> At both temperatures,  $\text{Al}_2\text{O}_3$  (and perhaps  $\text{AlNbO}_4$ ) is precipitated internally. At 900 °C, the  $\text{Al}_2\text{O}_3$  cannot form a continuous layer whereas at 1140 °C, a dense, continuous layer of  $\text{Al}_2\text{O}_3$  can form. The reason for this is that at lower temperatures  $J_{\text{alloy}}^{\text{Al}}$  is not sufficiently high to overcome  $J_{\text{oxide}}^{\text{Al}}$ , but as the temperature is increased,  $J_{\text{alloy}}^{\text{Al}}$  increases because of higher interdiffusion coefficients and at some time becomes greater than  $J_{\text{oxide}}^{\text{Al}}$ .

Clearly, the oxidation mechanism is more complex than that outlined above since the formation of nickel islands at 900 °C and  $\text{NiNb}_2\text{O}_6$  at 1140 °C has not been discussed. Pure nickel primarily forms at 900 °C due to the reduction of NiO by niobium atoms. At 1140 °C, the oxygen activity in the gas phase is sufficient to oxidize the niobium to  $\text{Nb}_2\text{O}_5$ , so  $\text{NiNb}_2\text{O}_6$  can form by reaction of NiO with  $\text{Nb}_2\text{O}_5$ .

## CONCLUSIONS

The following conclusions can be made regarding the role of the surface composition and the microstructure on the oxidation behavior of aluminide-coated  $\gamma/\delta$  directional eutectics:

1. The coating process variables have a marked effect on the oxidation behavior of aluminide-coated  $\gamma/\delta$  directional eutectics. The reason for this effect is the variety of surface compositions and coating microstructures that are produced by changing the process variables and it is these that alter the oxidation behavior. Consequently, once a microstructure has been obtained within specific composition limits, the oxidation behavior will be the same within those limits, irrespective of the combination of the processing variables utilized in obtaining the microstructure.

2. The oxidation behavior of the coated and uncoated  $\gamma/\delta$  directional eutectics was divided into three groups, depending on their surface composition. Coatings in Group I formed scales consisting solely of  $\text{Al}_2\text{O}_3$  and possessed the best oxidation resistance of the three groups. Coatings in Group II formed external scales of a niobium-rich oxide with an internal layer of  $\text{Al}_2\text{O}_3$ . These coatings possessed intermediate oxidation resistance. Substrates belonging to Group III formed an external scale of NiO and a zone of internal oxidation, and had the least oxidation resistance of the three groups.

3. The formation and the maintenance of the external scale was explained in terms of Wagner's criterion for external scale formation and by the relative magnitude of the diffusive fluxes of the element being oxidized in the coating (or substrate) and that consumed due to oxidation.

4. The coating microstructure affected the oxidation behavior within each group. Coatings with a single-phase layer had superior oxidation resistance to those with a two-phase lamellar morphology, in the same group.

5. Homogenization treatments favored the formation of a single-phase surface layer and so tended to increase oxidation resistance. Short-term anneals in argon (with

a low partial pressure of oxygen) prior to oxidation in air (pretreatments) favored the formation of the least noble element oxide ( $\text{Al}_2\text{O}_3$ ), thereby increasing the oxidation resistance.

## ACKNOWLEDGMENTS

The authors greatly appreciate the financial support of the Metallurgy Branch of the Office of Naval Research. They also wish to thank Mr. Sonny Knight, Saginaw Steering Division, General Motors Corporation, Saginaw, Michigan, for his assistance in quantitative scanning electron microscopy. Support from the Materials Research Laboratory Section, Division of Materials Research, National Science Foundation through use of central research facilities is also gratefully acknowledged.

## REFERENCES

1. E. J. Felten and F. S. Pettit: *Failure Modes in Composites-II*, J. N. Mehan and R. L. Fleck, eds., p. 220, AIME-IMD, New York, 1974.
2. J. Smeggil: AFML-TR-75-133, G. E. Corp. Res. Dev., Schenectady, NY, August 1975.
3. E. J. Felten, T. E. Strangman, and N. E. Ulion: NASA CR-134735, Pratt and Whitney Aircraft, East Hartford, CT, October 1974.
4. J. R. Rairden and M. R. Jackson: NAS-3-17815, G. E. Corp. Res. Dev., Schenectady, NY, July 1976.
5. T. E. Strangman, E. J. Felten, and R. S. Benden: NASA CR-135103, Pratt and Whitney Aircraft, East Hartford, CT, October 1976.
6. *High-Temperature Oxidation-Resistant Coatings*, ISBN 0-309-01769-6, NAC, Nat. Mat. Adv. Board, Washington, D.C., 1970.
7. S. J. Grisaffe: *The Superalloys*, C. T. Sims and W. C. Hagel, eds., p. 341, John Wiley & Sons, New York, 1972.
8. C. A. Krier and J. M. Gunderson: *Met. Eng. Q.*, 1965, vol. 5, pp. 1-16.
9. K. K. Yee: *Int. Metall. Rev.*, 1978, vol. 23, pp. 19-42.
10. H. C. Bhedwar, R. W. Heckel, and D. E. Laughlin: *J. Thin-Solid Films*, 1977, vol. 45, pp. 357-66.
11. G. W. Goward and D. H. Boone: *Oxid. Met.*, 1971, vol. 3, pp. 475-95.
12. P. N. Walsh: *Chemical Vapor Deposition, Fourth Intl. Conf.*, G. F. Wakefield and J. M. Blocker, Jr., eds., p. 147, Electrochem. Soc., Princeton, NJ, 1970.
13. S. R. Levine and R. M. Caves: *J. Electrochem. Soc.*, 1974, vol. 121, pp. 1051-64.
14. H. C. Bhedwar: Ph.D. Thesis, Carnegie-Mellon University, Pittsburgh, PA.
15. D. Laguitton, R. Rousseau, and F. Claise: *Anal. Chem.*, 1975, vol. 47, pp. 2174-78.
16. C. Wagner: *Z. Elektrochem.*, 1959, vol. 63, pp. 772-82.
17. P. Kofstad: *High Temperature Oxidation of Metals*, p. 112, John Wiley & Sons, New York, 1966.
18. R. E. Mistler and R. L. Coble: *J. Am. Ceram. Soc.*, 1971, vol. 54, pp. 60-61.
19. Y. Oishi and W. D. Kingery: *J. Chem. Phys.*, 1960, vol. 33, pp. 480-86.
20. G. Raison and A. Vignes: *Rev. de Phys. Appliquée*, 1970, vol. 5, pp. 535-44.
21. J. G. Smeggil and M. D. McConnell: *Oxid. Met.*, 1974, vol. 8, pp. 309-41.
22. J. G. Smeggil: *Oxid. Met.*, 1975, vol. 9, pp. 31-44.
23. K. Fueki and J. B. Wagner: *J. Electrochem. Soc.*, 1965, vol. 112, pp. 384-88.
24. E. R. Thompson and F. D. Lemkey: *Trans. ASM*, 1966, vol. 62, pp. 140-54.
25. E. R. Thompson, E. H. Kraft, and F. D. George: Final Report UARL, Contract N00019-71-C-0096, United Aircraft Research Laboratory, East Hartford, CT, July 1971.